# Metal π complexes of benzene derivatives
# Part 57. *p*-Phenylenediamine as a sandwich-complex ligand[☆]

Christoph Elschenbroich *, Mathias Pietras, Klaus Harms

*Fachbereich Chemie der Philipps-Universität Marburg, Hans-Meerwein-Strasse, D-35032 Marburg, Germany*

Dedicated to Professor Ernst Otto Fischer on the occasion of his 85th birthday

## Abstract

Metal-atom ligand-vapor cocondensation affords the sandwich complexes di[1,4-bis(trimethylsilylamino)-$\eta^6$-benzene]chromium (**4**) and di[1,4-bis(dimethylamino)-$\eta^6$-benzene]chromium, $(TMPD)_2Cr$ (**5**). In the crystal **4** adopts an eclipsed structure with intramolecular, interannular N–H···N hydrogen bonds. $\mathbf{5^{+\bullet}I^-}$ in the crystal forms staggered, synclinal cations $\mathbf{5^{+\bullet}}$ (twist angle 31°) featuring boat distortions of the $\eta^6$-arenes and displacements of the N atoms away from the central metal atoms. This deformation is virtually absent in the structure of **4**. According to EPR spectroscopy, in rigid solution the cations $\mathbf{5^{+\bullet}}$ relax to a twist angle of 45°. Cyclic voltammetry performed on **5** points to the oxidation sequence $(TMPD)_2Cr \underset{-e^-}{\overrightarrow{\phantom{-}}} [(TMPD)_2Cr]^{+\bullet} \underset{-e^-}{\overrightarrow{\phantom{-}}} [(TMPD)_2Cr]^{2+} \rightarrow Cr^{2+}(solv) + 2\,TMPD \underset{-2e^-}{\overrightarrow{\phantom{-}}} 2\,TMPD^{+\bullet} \underset{-2e^-}{\overrightarrow{\phantom{-}}} 2\,TMPD^{2+}$, which, in part, can be monitored by EPR spectroscopy (observation of $(TMPD)_2Cr^{+\bullet}$ and $TMPD^{+\bullet}$). The potential $E_{1/2}(\mathbf{5^{+/0}})$ is the most cathodic one ever reported for a bis(arene)metal complex.
© 2003 Elsevier B.V. All rights reserved.

*Keywords:* Bis(arene)metal complexes; *N,N,N′,N′*-Tetramethyl-*para*-phenylenediamine (TMPD); Structural distortion; Cyclic voltammetry; EPR spectroscopy; Hydrogen bonding

## 1. Introduction

*para*-Phenylenediamine and its *N*-alkyl derivatives possess a number of interesting properties. As mild reductants they are easily converted into very stable, highly colored radical cations (Wurster's Red, Wurster's Blue [2]) which are amenable to EPR spectroscopic study [3]. Radical salts, formed with the radical anions which arise from the respective oxidizing agent are of interest in the context of electric conductivity [4] and molecular magnetism [5]. Being a comparatively weak electron donor *N,N,N′,N′*-tetramethyl-*para*-phenylene-diamine (TMPD) in solvents of low polarity forms diamagnetic charge-transfer complexes, whereas in solvents of higher polarity electron transfer occurs [6]. As

potential ligands phenylenediamines are ambidentate in that metal coordination via the amino groups, via the aromatic π-electron system, or a combination of both variants, is conceivable.

Since metal-vapor synthesis is a kinetically controlled process, it appeared interesting to explore questions of site selectivity of coordination. The consequences of metal complex formation on the aforementioned properties of the ligands are also worth probing. Assessments of the effect of metal coordination on ligand properties are more appropriate for bis(arene)metal- than for di(cyclopentadienyl)metal complexes since in the former class the free ligand and its π-complex have the same charge and spin multiplicity. Contrarily, neutral, closed shell ferrocene may be formally disected into $Fe^{2+}$ and $C_5H_5^-$ or into $Fe^0$ and $C_5H_5^\bullet$. Nevertheless, the ferrocenylamines may serve as an inspiration for synthetic paths towards amino derivatives of bis(arene)metal complexes. Interestingly, despite their inception in the late 1950s [7] the ferrocenylamines have been some-

---

what problematic due to lack of simple, high-yield methods of preparation and their susceptibility to air-oxidation at the N−H bond [8]. The situation has been remedied by a recent, improved synthesis and full characterization of 1,1′-diaminoferrocene [9]. More extensive studies have been performed on alkylamino-ferrocenes, which have been prepared in large variety and used as chelating ligands [10].

Less abundant than the aminometallocenes are bis-(arene)metal complexes carrying amino groups as peripheral substituents. We have reported on the parent complex bis($\eta^6$-aniline)chromium in 1993 [11], dimethyl-amino derivatives had been known for some time [12,13]. This paper describes an extension to *para*-phenylenediamines as ligands to chromium. Questions to be addressed, inter alia, deal with the redox ambiguity inherent in the fact that in a bis(*para*-phenylenediamine)chromium complex the central metal as well as the ligand could be the site of oxidation and the role N−H···N hydrogen bonding may play in governing the structure. An interesting perspective is the potential use of *para*-phenylenediamine sandwich complexes as chelating bridging ligands in redox active coordination polymers, isolation of the target compounds in sufficient quantity permitting.

## 2. Results and discussion

Simply trying to transfer protocols of aminoferrocene synthesis to the preparation of bis(*para*-phenylenediamine)chromium derivatives is unavailing since the former starts with a lithiation step and regioselective 1,4,1′,4′-tetralithiation of bis(benzene)chromium (1) is impractical. As in the case of bis($\eta^6$-aniline)chromium, we reverted to metal-atom ligand-vapor cocondensation techniques (CC). Bis(arene)metal complexes bearing NH$_2$ groups cannot be obtained directly by CC, rather N(SiMe$_3$)$_2$-derivatives must first be prepared with desilylation to follow [11]. However, probably for steric reasons, cocondensation of N,N,N′,N′-tetrakis(tri-methylsilyl)-*para*-phenylenediamine vapor with chromium vapor failed to yield the expected sandwich complex. Contrarily, the presence of the substituents − NH(SiMe$_3$) and −NMe$_2$ allowed the low-yield syntheses of the respective bis(*para*-phenylenediamine)chromium complexes 4 and 5 (Scheme 1).
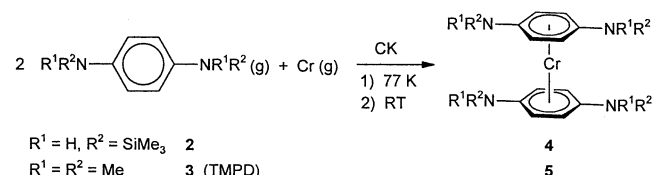
Di[1,4-bis(trimethylsilylamino)-$\eta^6$-benzene]chromium (4) and di[1,4-bis(dimethylamino)-$\eta^6$-benzene)]chromium (5) are reddish brown, sublimable, highly air-sensitive materials which are soluble in most of the common organic solvents. Desilylation of 4 to yield the parent complex which contains four NH$_2$ groups failed, presumably because the precursor 4 could be isolated on a 10 mg scale only. Somewhat better yields (100 mg scale) were reached for 5. The low yield of 4 is unfortunate because in the case of bis(trimethylsilyla-mino-$\eta^5$-cyclopentadienyl)iron double deprotonation yields a quite versatile, ferrocene-containing bisamido ligand [14].

The structure of 4 in the crystal is of interest, however, in that intramolecular interligand N−H···N hydrogen bonding generates an eclipsed conformation rendering the coordination sphere of the chromium atom reminiscent of a [3.3]paracyclophane (Fig. 1). Formation of intramolecular hydrogen bonds may also explain the fact that the nitrogen atoms and the *ipso*-carbon atoms
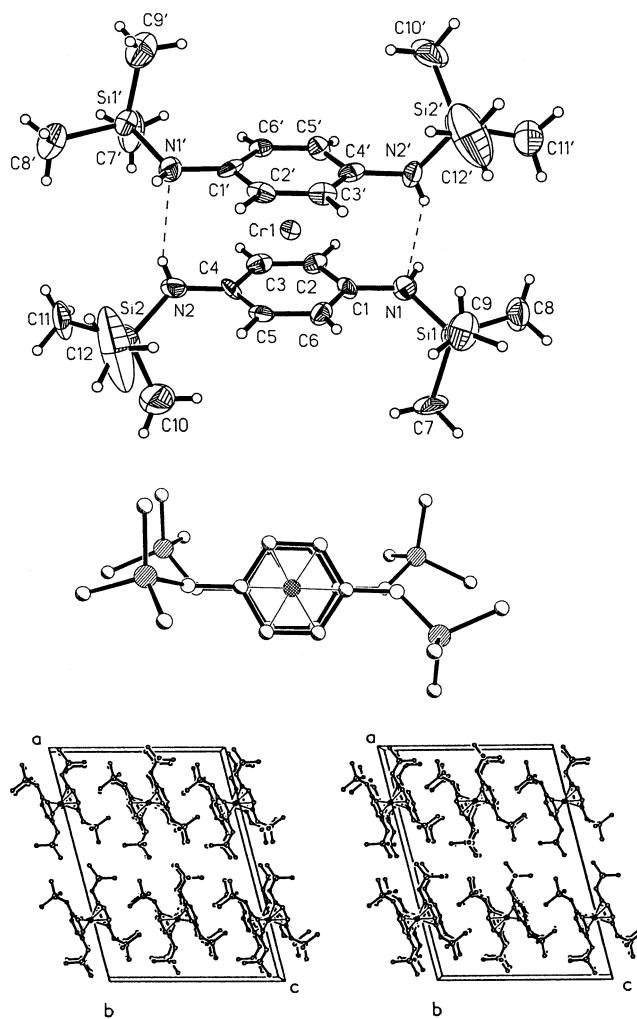


Fig. 1. Di[1,4-bis(trimethylsilylamino)-$\eta^6$-benzene]chromium (4): PLA-TON representation (thermal ellipsoids indicate 50% probability levels), eclipsed conformation in the crystal and packing diagram (stereoplot).



2 R$^1$R$^2$N-⟨⟩-NR$^1$R$^2$ (g) + Cr (g)  →  complexes 4 / 5

R$^1$ = H, R$^2$ = SiMe$_3$   2
R$^1$ = R$^2$ = Me   3 (TMPD)

4
5

Scheme 1.

are bent away from the central chromium atom to a smaller extent than is usually the case for ($\eta^6$-arene) metal complexes bearing peripheral $\pi$-donor substituents [15]. In Fig. 2 the respective distortion parameters are defined, they are compared with those in di[1,4-bis(dimethylamino)benzene]chromium iodide ($\mathbf{5}^+ I^-$) and in the half-sandwich complex [1,4-bis(dimethylamino)benzene](tricarbonyl)chromium (**6**) in Table 1. Structural features of interest for $\eta^6$-*para*-phenylenediamines also include the degree of pyramidalicity of the nitrogen environment, the $C_{ipso}$–N bond lengths and C–C bond alternation within the six-membered ring, properties which are interrelated. For the complex **4** the sums of the angles about the amine nitrogen atoms (N1 360°, N2 360°, N1′ 350°, N2′ 360°) point at little or no deviation from trigonal planarity of the N(C,Si,H) segments. The high steric demand of the SiMe$_3$ groups and the steric requirements for N–H$\cdots$N hydrogen bonding enforce two types of conformation of the $C_{ipso}$–N(Si,H) bonds: the twists about C1–N1 and C1′–N1′ place the lone pairs and those about C4–N2 and N4′–N2′ the N–H bonds in positions appropriate for N–H$\cdots$N hydrogen bonding. Conjugation of the nitrogen lone pairs with the aromatic $\pi$-systems is thereby reduced and the $C_{ipso}$–N bond lengths of 143 pm (average) deviate only to a small extent from that of a C–N single bond [compare: d(C–N) 147 pm, d(C=N) 130 pm]. Consequently, no bond alternation in the arene is observed which would point at the possible contribution of quinoid valence bond structures.

The structure of $\mathbf{5}^+ \cdot I^-$ in the crystal (Fig. 2) differs from that of **4** in a number of ways. (Crystals suitable for X-ray diffraction could only be obtained for the iodide of the cationic complex.) Based on the torsional angle with regard to the sandwich axis of 31°, the staggered conformation, which the cation in $\mathbf{5}^+ \cdot I^-$ adopts in the crystal, may be designated as synclinical. Displacement of the $C_{ipso}$- and N atoms away from the central metal atom is more pronounced for $\mathbf{5}^+ \cdot I^-$ compared to **4** (Table 2). As in **4**, except for N2, the environment of the N atoms in $\mathbf{5}^+ \cdot I^-$ is virtually trigonally planar as inferred from the angle sums (N1 358.4°, N2 351.0°, N1′ 358.4°, N2′ 359.8°). Coplanarity of the dimethylamino groups with the best planes spanned by the arene carbon atoms provides for $C_{ipso}$–N conjugation. Correspondingly, the $C_{ipso}$–N bonds for $\mathbf{5}^+ \cdot I^-$ (138 pm, average) are markedly shorter than in **4**, thereby reflecting a higher C,N double bond character. Nonetheless, alternating C,C bond lengths in the arene ring are not discernible. This contrasts with the structure of [TMPD]$^+$ClO$_4^-$ (Wurster's Blue perchlorate), in which a long–short–long pattern for the $C_{ipso}$CCC$_{ipso}$ segments is manifest [16]. Obviously, $\eta^6$-coordination serves to counteract the N,$C_{ipso}$-conjugation induced tendency for bond length

alternation. Selected bond lengths, which illustrate these statements, are collected in Table 2.

## 2.1. Redox properties

The complexes **4** and **5** contain two sites which may be subject to oxidation, i.e. the central chromium atom and the *para*-phenylenediamine ligand. If these components are viewed as separate entities, the potentials $E_{1/2}[(C_6H_6)_2Cr^{+/0}] = -0.68$ V [17] and $E_{1/2}[TMPD^{+/0}] = 0.20$ V [18] must be considered. Clearly, primary oxidation at chromium is expected to take place because the gradation of 0.83 V is too large for a coordination-induced shift of the primary oxidation site from chromium to the *para*-phenylenediamine to occur. Contrarily, the electron donating character of the peripheral amino groups produces strong cathodic shifts of the potentials $E_{1/2}(\mathbf{4}^{+/0})$ and $E_{1/2}(\mathbf{5}^{+/0})$ relative to the parent bis(benzene)chromium$^{+/0}$ couple. In fact, $E_{1/2}(\mathbf{5}^{+/0}) = -1.15$ V (vs SCE) constitutes the most negative value ever reported for a bis($\eta^6$-arene)chromium complex. For the cyclovoltammetric traces and the electrochemical parameters of **5** see Fig. 3. The large potential-range CV points to at least five redox steps, 3 and 5 displaying reversibility. In the limited scan range $-1.5$ V $< E < 0$ V wave 2 appears reversible as well. While wave 1 unquestionably signalizes primary chromium oxidation ($\mathbf{5}^{+/0}$) 2 could either stem from secondary chromium oxidation or from ligand oxidation. We exclude the second alternative because a cathodic shift of the oxidation potential of a ligand bonded to a metal cation is unreasonable. Wave 2 is therefore assigned to the couple $\mathbf{5}^{2+/+}$. Precedent for [($\eta$-arene)$_2$Cr]$^{2+}$ dications is very limited because these species are prone to nucleophilic ligand displacement. Typically, reversible secondary oxidation had been observed only when nucleophilic attack is blocked by extensive substitution, as in bis(hexamethylbenzene)chromium, or if the chelate effect stabilizes the sandwich-complex dication as in ($\eta^{12}$-[2.2]paracyclophane)chromium [17,19]. Accordingly, attempts to prepare salts $\mathbf{5}^{2+}(X^-)_2$ were unsuccessful. Rather, chemical oxidation of **5** by dioxygen generates a blue solution which in a CV experiment fails to exhibit the waves at $-1.15$ and $-0.30$ V, the waves at more positive potential are maintained, however. Obviously, chemical oxidation to $\mathbf{5}^{2+}$ is followed by ligand displacement, and further oxidation of the free ligand generates Wurster's Blue radical cation TMPD$^{+\cdot}$ as also supported by EPR spectroscopy (vide infra).

Chemical irreversibility of the second oxidation step is demonstrated in CV by the fact that for scan rates lower than 20 mV s$^{-1}$ the peak current ratio $r = i_c/i_a$ is smaller than unity. In the faster scan regime, the electrochemical data for the couple $\mathbf{5}^{2+/+}$ point to quasi-reversible character in that the peak separation $\Delta E_p$ increases with
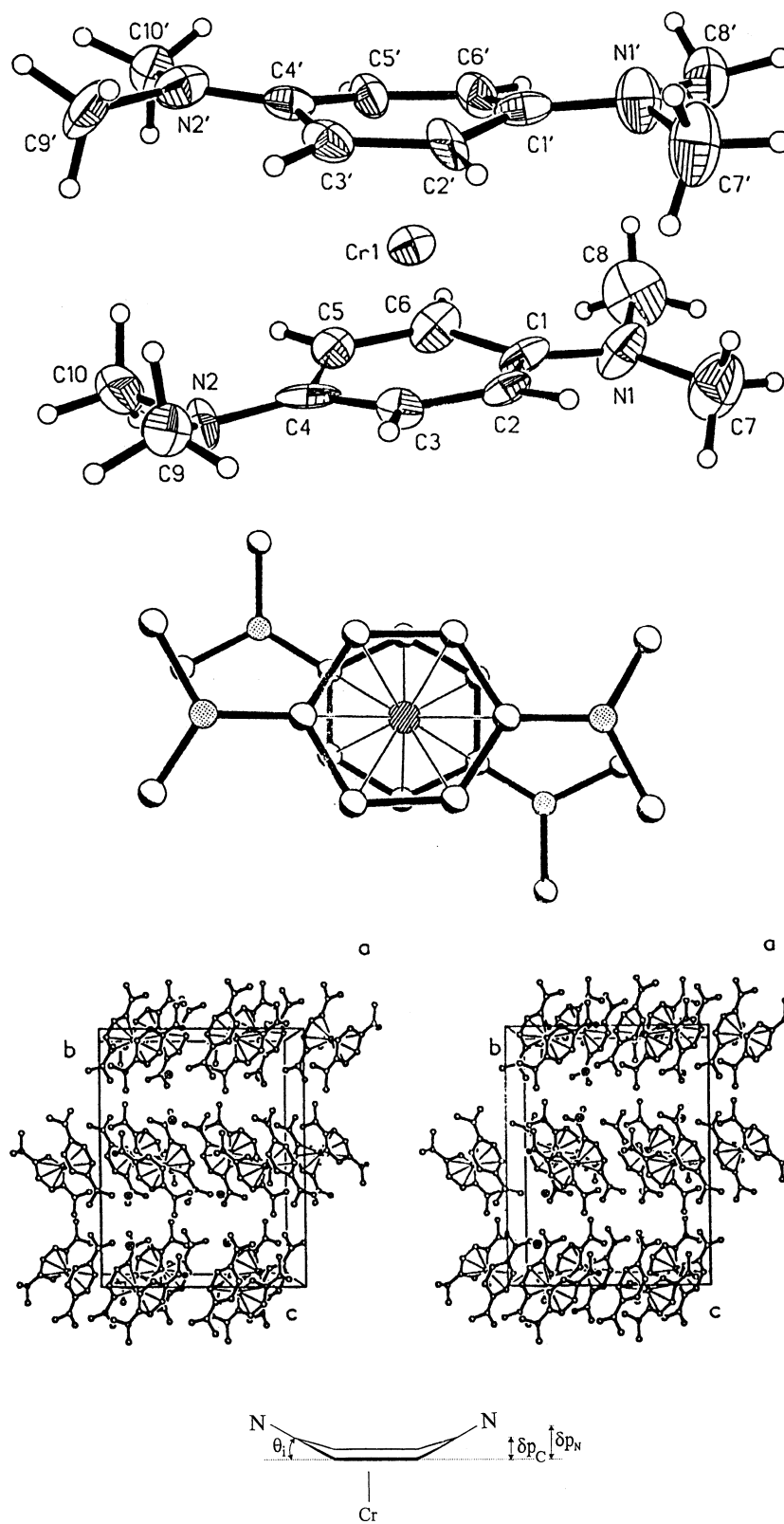
Fig. 2. Di[1,4-bis(dimethylamino)-$\eta^6$-benzene]chromium iodide $\mathbf{5}^+\mathbf{I}^-$: PLATON representation (thermal ellipsoids indicate 50% probability levels), staggered conformation in the crystal and packing diagram (stereoplot). The definitions of the ligand distortion parameters $\Theta_i$, $\delta_\mathrm{C}^\mathrm{P}$ and $\delta_\mathrm{N}^\mathrm{P}$ are also given.

Table 1
Comparison of the ligand distortion parameters $\Theta_i$ (deg), $\delta_C^P$, and $\delta_N^P$ (pm) and the C,N-bond lengths for the complexes **4**, **5$^+$·I$^-$**, and **6**; these parameters are defined in Fig. 2

|  | $\Theta_i$ | $\delta_C^P$ | $\delta_N^P$ | d(C$_{ipso}$–N) |
|---|---|---|---|---|
| (**6**) (Me$_2$NC$_6$H$_4$NMe$_2$)Cr(CO)$_3$ | 6 | 8 | 20 | 131 |
| (**5**) (Me$_2$NC$_6$H$_4$NMe$_2$)$_2$CrI | 10 | 14 | 28 | 138 |
| (**4**) [(Me$_3$Si)(H)NC$_6$H$_4$N(H)(SiMe$_3$)]$_2$Cr | 1–2 | 2 | 3 | 143 |

Mean values are given here, for individual deviations from coplanarity see Section 5.

the scan rate [$v$ (mV s$^{-1}$), $\Delta E_p$ (mV): 20, 43; 50, 69; 100, 93; 200, 170]. Four dimethylamino substituents do not provide complete steric shielding of the central metal atom/ion against nucleophilic attack. Therefore, the fact that secondary oxidation can be observed by CV at all must be traced to the strong electron donating effect of the NMe$_2$ substituents, which decreases the electrophilicity of the central metal. Note that, conversely and apart from steric considerations, electron accepting peripheral substituents render [bis(arene)chromium(I)]$^+$ cations highly substitution-labile [20].

It remains to comment on the CV waves following those attributed to the couples **5$^{+/0}$** and **5$^{2+/+}$**. In the positive scan range $0 < E < 1.0$ V two waves whose features ($\Delta E_p$, $r$) approach reversibility and two shoulders are observed. Waves 3 and 5 of the CV trace are assigned to the oxidation of the free ligand TMPD, which is released in the cleavage of the dication **5$^{2+}$**. These potentials correspond to the values reported for free TMPD [18]. The comparatively large peak currents for 3 and 5, relative to those in 1 and 2 are in line with
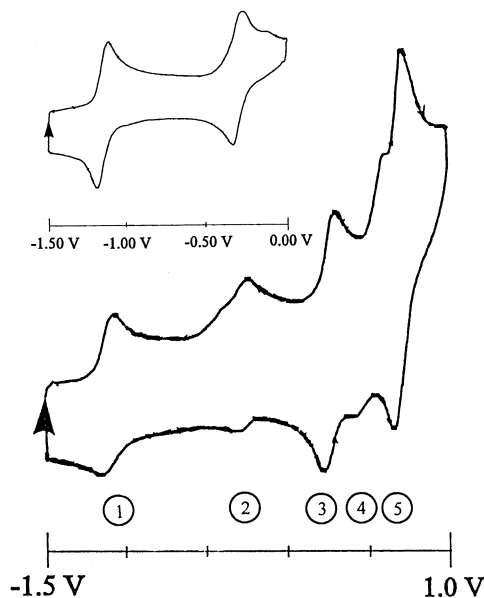
Fig. 3. Cyclic voltammogram of di[1,4-bis(dimethylamino)-η$^6$-benzene]chromium (**5**) in dimethoxyethane, $n$-Bu$_4$NClO$_4$, vs. SCE, at $-40$ °C, $E_p$ (V), $\Delta E_p$ (mV). 1: $E_{pa} = -1.10$, $E_{pc} = -1.19$, $\Delta E_p = 85$, $r = i_a/i_c > 1$; 2: $E_{pa} = -0.26$, $E_{pc} = -0.34$, $\Delta E_p = 75$, $r > 1$; 3: $E_{pa} = 0.18$, $E_{pc} = 0.24$, $\Delta E_p = 62$, $r \approx 1$; 4: $E_{pa} = 0.63$, $E_{pc} = 0.47$, $\Delta E_p = 165$; 5: $E_{pa} = 0.76$, $E_{pc} = 0.70$, $\Delta E_p = 62$, $r \approx 1$. Limited scan range $-1.5 < E < 0$ V (inset): 1: $E_{pa} = -1.19$, $E_{pc} = -1.12$, $\Delta E_p = 70$, $r = 1$; 2: $E_{pa} = -0.33$, $E_{pc} = -0.27$, $\Delta E_p = 65$, $r = 1$.

the assignment because cleavage of one unit of **5** generates two electrochemically active free TMPD ligands. Furthermore, the diffusion coefficients for complex **5** and ligand TMPD most likely differ. We exclude the possibility that the wave 3 arises from the oxidation of chromium-coordinated TMPD. This no-

Table 2
Selected bond lengths (Å) in the complexes **4** and **5$^+$·I$^-$**
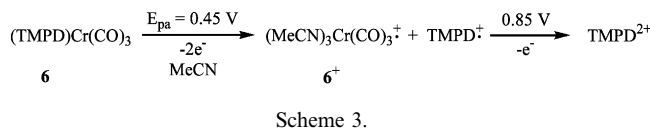
|  | **4** | **5$^+$·I$^-$** |  | **4** | **5$^+$·I$^-$** |
|---|---|---|---|---|---|
| C(1)–C(2) | 1.401(10) | 1.413(15) | Cr(1)–C(1) | 2.162(8) | 2.278(12) |
| C(1)–C(6) | 1.403(11) | 1.451(16) | Cr(1)–C(2) | 2.133(7) | 2.137(10) |
| C(2)–C(3) | 1.410(9) | 1.406(15) | Cr(1)–C(3) | 2.132(7) | 2.138(11) |
| C(3)–C(4) | 1.398(10) | 1.432(15) | Cr(1)–C(4) | 2.169(7) | 2.283(13) |
| C(4)–C(5) | 1.388(11) | 1.415(16) | Cr(1)–C(5) | 2.150(7) | 2.153(11) |
| C(5)–C(6) | 1.435(10) | 1.454(16) | Cr(1)–C(6) | 2.149(7) | 2.164(11) |
| C(1′)–C(2′) | 1.406(10) | 1.376(15) | Cr(1)–C(1′) | 2.184(7) | 2.286(12) |
| C(1′)–C(6′) | 1.400(11) | 1.417(15) | Cr(1)–C(2′) | 2.139(7) | 2.124(10) |
| C(2′)–C(3′) | 1.404(9) | 1.410(15) | Cr(1)–C(3′) | 2.128(7) | 2.168(11) |
| C(3′)–C(4′) | 1.415(10) | 1.426(15) | Cr(1)–C(4′) | 2.120(8) | 2.325(11) |
| C(4′)–C(5′) | 1.411(11) | 1.415(15) | Cr(1)–C(5′) | 2.140(7) | 2.127(12) |
| C(5′)–C(6′) | 1.404(9) | 1.388(15) | Cr(1)–C(6′) | 2.144(6) | 2.143(11) |
| C(1)–N(1) | 1.426(9) | 1.398(15) | N(2)–H(20)···N(1′) |  | 3.189(9) |
| C(4)–N(2) | 1.412(11) | 1.372(15) | N(2)–H(20) |  | 0.73(6) |
| C(1′)–N(1′) | 1.413(10) | 1.387(14) | H(20)···N(1′) |  | 2.74(6) |
| C(4′)–N(2′) | 1.443(11) | 1.361(14) | < N(2) H(20) N(1′) |  | 123(6)° |
|  |  |  | N(2′)–H(20′)···N(1) |  | 3.176(9) |
|  |  |  | N(2′)–N(20′) |  | 0.81(6) |
|  |  |  | H(20′)···N(1) |  | 2.46(6) |
|  |  |  | < N(2′) H(20′) N(1) |  | 148(6)° |

tion is supported by the limited reversibility of the couple $5^{2+/+}$ and by the expectation that TMPD coordinated to $Cr^{2+}$ should display a large anodic shift of the potential $E(TMPD^{+/0})$, contrary to observation in the present case. The barely resolved irreversible wave 4 may be caused by $Cr^{2+}$(solv) oxidation, no corroborative evidence being available, however. The sequence of events during electrochemical oxidation of **5** therefore appears to be as shown in Scheme 2.

It is of interest to look at the electrochemical oxidation of the half-sandwich complex ($\eta^6$-Me$_2$NC$_6$H$_4$NMe$_2$)Cr(CO)$_3$(**6**) for comparison [18] (Scheme 3) **5** and **6** differ in that for the half-sandwich complex **6** primary oxidation occurs at a potential between the potentials for primary and secondary oxidation of free TMPD. Therefore, the anodic peak $E_{pa} = 0.45$ V signalizes the three processes $6^{+/0}$, ligand displacement at $6^+$ and TMPD$^{+/0}$. Contrarily, because of the much more cathodic region for the oxidation of the sandwich complex **5**, the four steps $5^{+/0}$, $5^{2+/+}$, TMPD$^{+/0}$ and TMPD$^{2+/+}$ are well resolved on the potential axis.

Consequently, paramagnetic intermediates in the chain of electron transfer steps for **5** may be identified by EPR spectroscopy. Mild oxidizing agents like 4-pyridine carbaldehyde generate the complex radical cation $5^{+\bullet}$, air-oxidation of the latter causes a color change from red to blue due to the formation of the ligand radical cation TMPD$^{+\bullet}$. EPR spectra are depicted in Fig. 4, the respective parameters are collected in Table 3. Whereas the EPR data for TMPD$^{+\bullet}$ are identical to those reported previously [3], a few comments on the EPR data for the new radical cation $5^{+\bullet}$ will be given. Hyperfine coupling to 8 $^1$H and 1 $^{53}$Cr is resolved in the isotropic spectrum of $5^{+\bullet}$; splittings caused by 4 $^{14}$N are not discernible. EPR silence of non-hydrogen magnetic nuclei in the periphery of paramagnetic bis(arene)metal complexes has been noted in the past, no satisfactory explanation being available.

As commonly observed, electron donating peripheral substituents cause an increase in the coupling constant $a(^1H)$ at the expense of $a(^{53}Cr)$. Therefore, it does not come as a surprise that $a(8\ ^1H, 5^{+\bullet}) = 0.456$ mT is the largest value ever registered for a [bis(arene)Cr]$^{+\bullet}$

$$(TMPD)Cr(CO)_3 \xrightarrow[\substack{-2e^- \\ MeCN}]{E_{pa}\,=\,0.45\ V} (MeCN)_3Cr(CO)_3^{\cdot+} + TMPD^{\cdot+} \xrightarrow[-e^-]{0.85\ V} TMPD^{2+}$$
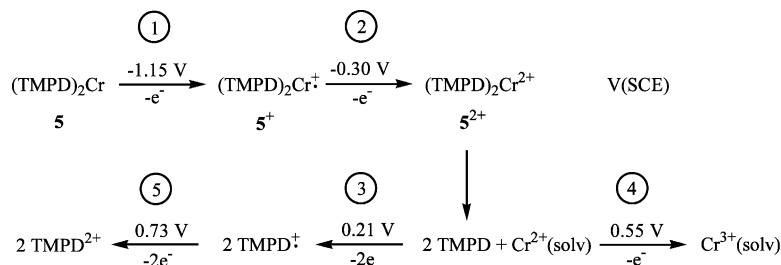$$\mathbf{6} \qquad\qquad\qquad\qquad \mathbf{6^+}$$

Scheme 3.

radical cation; correspondingly, $a(^{53}Cr) = 1.696$ mT is fairly small. This phenomenon may be rationalized by decreased $Cr^{\delta+}$ charge in $5^{+\bullet}$, induced by 4 electron-donating NMe$_2$ groups, attendant expansion of the SOMO Cr $3d_{z^2}$ and more effective spin polarization of the C–H bonds. The exceptionally well resolved spectrum of $5^{+\bullet}$ in rigid solution is indicative of tetragonal symmetry ($g_x = g_y = g_\perp$). Therefore, as opposed to the crystalline state, in rigid solution $5^{+\bullet}$ predominantly exists as the rotamer with a 90° angle of twist along the sandwich axis. Obviously, the conformation of the cation $5^{+\bullet}$ in the crystal is dominated by packing forces, whereas in rigid solution the conformation adopted is such as to minimize intramolecular repulsion.

## 3. Experimental

Chemical manipulations and physical measurements were carried out using techniques and instruments specified previously [21]. The ligands 1,4-bis(trimethylsilylamino)benzene (**2**) [22] and 1,4-bis(dimethylamino)benzene (**3**) [23] were prepared according to literature methods. Metal-atom ligand-vapor cocondensations were performed in a 4 l reactor cooled with liquid dinitrogen and equipped with a heatable ligand inlet tube and a conical tungsten spirale (wire diameter 1 mm) for chromium evaporation. Chromium sand (0.5–2.0 mm) provided by Heraeus was used.

### 3.1. [1,4-(Me$_3$SiNH)$_2$-$\eta^6$-C$_6$H$_4$]$_2$Cr (4)

1,4-(Me$_3$SiNH)$_2$C$_6$H$_4$ (16 g, 0.064 mol) and Cr (1.2 g, 0.023 mol) were cocondensed in a 4 l reactor at $5 \times 10^{-4}$ mbar, metal evaporation being effected by 5V/38A applied to the source. Start of ligand evaporation preceded that of metal evaporation by 15 m in order to cover the reactor surface by a thin layer of the ligand. Total cocondensation time was 1 h. The reactor was flooded with N$_2$ and allowed to warm to room

$$\begin{array}{ccccc}
& \textcircled{1} & & \textcircled{2} & \\
(TMPD)_2Cr & \xrightarrow[-e^-]{-1.15\ V} & (TMPD)_2Cr^{\cdot+} & \xrightarrow[-e^-]{-0.30\ V} & (TMPD)_2Cr^{2+} \qquad V(SCE) \\
\mathbf{5} & & \mathbf{5^+} & & \mathbf{5^{2+}} \\[2em]
& \textcircled{5} & & \textcircled{3} & \qquad\qquad \textcircled{4} \\
2\ TMPD^{2+} & \xleftarrow[-2e^-]{0.73\ V} & 2\ TMPD^{\cdot+} & \xleftarrow[-2e]{0.21\ V} & 2\ TMPD + Cr^{2+}(solv) \xrightarrow[-e^-]{0.55\ V} Cr^{3+}(solv)
\end{array}$$

Scheme 2.

temperature. The dark reddish-brown cocondensate was dissolved in toluene and filtered through celite, the residue being washed with toluene until the filtrate was pale yellow. The solvent was removed in vacuo and the residue was heated to 120 °C to distill off excessive ligand. High-vacuum sublimation (135 °C, $10^{-4}$ mbar)
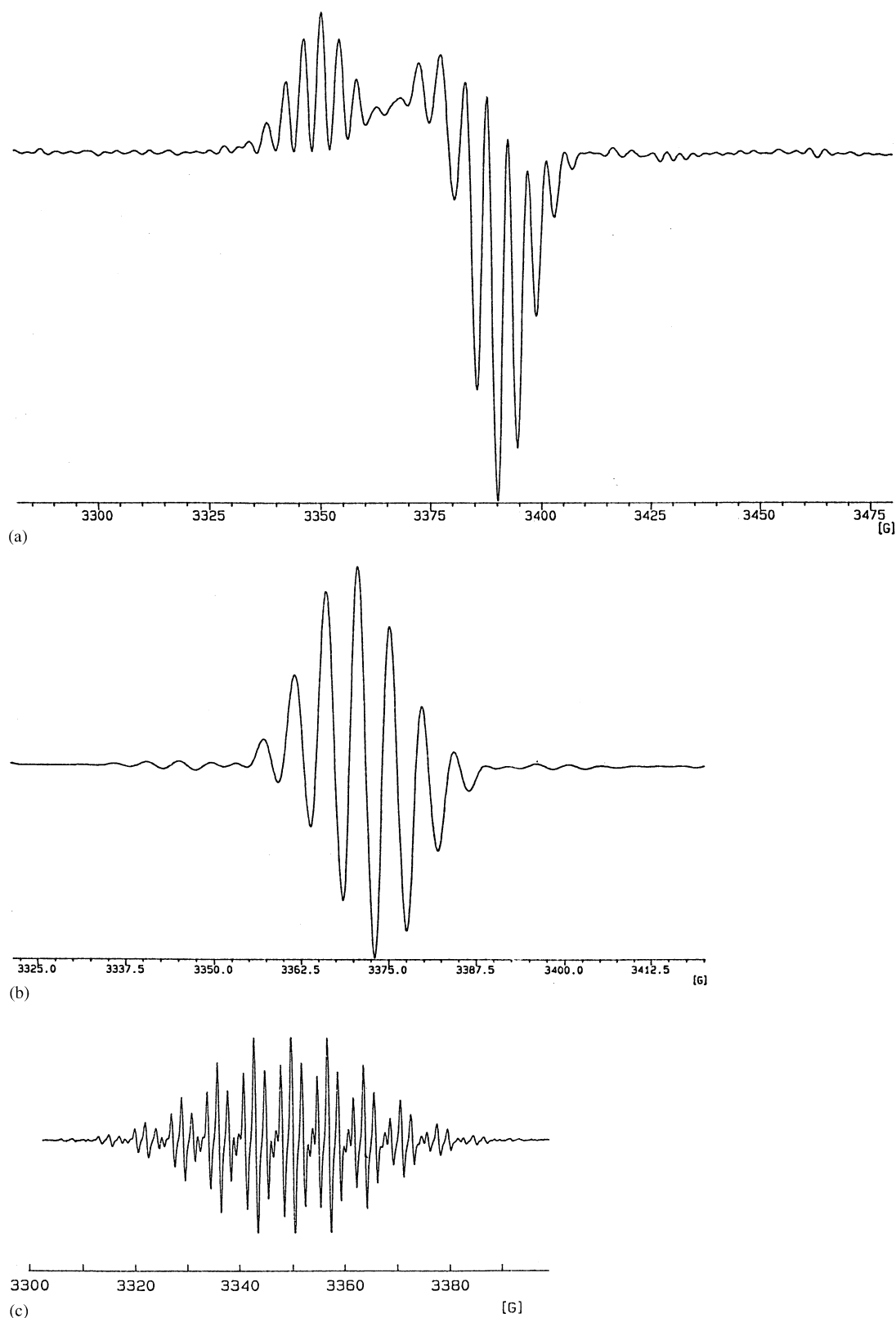


Fig. 4. EPR spectra (X-band) of the complex radical cation $\mathbf{5}^{+\bullet}$ in rigid solution (THF, 120 K, $\mathbf{a}$), in fluid solution (THF, 295 K, $\mathbf{b}$) and of the ligand radical cation $TMPD^{+\bullet}$ ($\mathbf{3}^{+\bullet}$, THF, 295 K, $\mathbf{c}$).

Table 3
EPR data for the complex radical cations $4^{+\cdot}$ and $5^{+\cdot}$ in fluid and in rigid solution [a]

|  | $4^{+\cdot}$ | $5^{+\cdot}$ |
|---|---|---|
| $\langle g \rangle$ | 1.9898 | 1.9905 |
| $g_{\parallel}$ | 2.0049 | 2.0057 |
| $g_{\perp}$ | 1.9834 | 1.9825 |
| $a(^1H)$ | 0.397 | 0.456 |
| $A_{\parallel}(^1H)$ |  | 0.393 |
| $A_{\perp}(^1H)$ |  | 0.480 |
| $a(^{53}Cr)$ | 1.734 | 1.696 |

[a] Solvent: THF, 295 K (fluid), 120 K (rigid). Coupling constants in mT.

afforded a small amount (30 mg, about 2 ‰) of **4** as reddish brown crystals.

Anal. Calc. for $C_{24}H_{48}CrN_4Si_4$ (556.99 g mol$^{-1}$): C, 51.75; H, 8.69; N, 10.06. Found: C, 51.86; H, 8.41; N, 10.34%. EIMS (70 eV) [$m/z$, %]: 556 [M$^+$, 4.2%], 304 [(M−L)$^+$, 19%], 252 [L$^+$, 100%], 237 [(L−Me)$^+$, 48%], 147 [PhNSiMe$_3^+$, 28%], 73 [SiM$_3^+$, 37%]. $^1$H-NMR (C$_6$D$_6$): $\delta$ 0.31 (12H, C$H_3$), 2.10 (4H, N$H$), 4.19 (8H, C$_6H_4$). $^{13}$C{$^1$H}-NMR (C$_6$D$_6$): 1.32 (CH$_3$, $J_{C-H} = 118.4$ Hz), 70.80 (C2,3,5,6, $J_{C-H} = 161.9$ Hz), 105.45 (C1,4).

### 3.2. [1,4-(Me₂N)₂-η⁶-C₆H₄]₂Cr (5)

1,4-(Me$_2$N)$_2$C$_6$H$_4$ (21 g, 0.13 mol) and Cr (1.5 g, 0.029 mol) were cocondensed in a 4 l reactor at $5 \times 10^{-4}$ mbar during 1.5 h, 5V/38A being applied to the metal evaporation source. It proved advantageous to generate thin layers of methylcyclohexane on the reactor surface prior to cocondensation and intermittently during cocondensation in order to facilitate removal of product. After termination of the cocondensation process and warming to ambient temperature the dark red solution of the reaction product was filtered through celite. The solvent was removed in vacuo and excessive ligand was distilled off at 80 °C. The residue was sublimed at 105 °C/10$^{-4}$ mbar to yield 520 mg (1.4 mmol, 5%) of **5** as a reddish-brown microcrystalline material.

Anal. Calc. for $C_{20}H_{32}CrN_4$ (380.50 g mol$^{-1}$): C, 63.13; H, 8.48; N, 14.72. Found: C, 63.42; H, 8.67; N, 15.14%. EIMS (70 eV) [$m/z$, %]: 380 [M$^+$, 4.9%], 216 [(M−L)$^+$, 5.9%], 164 [L$^+$, 100%], 149 [(L−Me)$^+$, 57%], 120 [(L−NMe$_3$)$^+$, 21%]. $^1$H-NMR (C$_6$D$_6$): $\delta$ 2.71 (24H, C$H_3$), 4.40 (8H, C$_6H_4$). $^{13}$C-NMR (C$_6$D$_6$): $\delta$ 42.17 (CH$_3$, $J_{C-N} = 133.8$ Hz), 64.10 (C2,3,5,6, $J_{C-H} = 165.3$ Hz), 117.63 (C 1,4).

### 3.3. {[1,4-(Me₂N)₂-η⁶-C₆H₄]₂Cr}PF₆ (5⁺·PF₆⁻)

To a solution of **5** (300 mg, 0.8 mmol) in 50 ml of tetrahydrofuran a solution of ($n$-Bu$_4$N)PF$_6$ (1.5 g, 4

mmol) in 20 ml of tetrahydrofuran was added. After stirring for 10 m at ambient temperature 0.6 ml of 4-pyridine carbaldehyde were added dropwise resulting in a color change from reddish-brown to carmine red. The mixture was stirred for 30 m, 50 ml of Et$_2$O were added, the resulting precipitate was collected and washed in Et$_2$O and water. Dissolving in the minimal amount of acetone (ca. 10 ml) and layering with Et$_2$O yielded $5^{+\cdot}$PF$_6$ (410 mg, 0.75 mmol, 95%) of a carmine red, highly air sensitive powder.

Anal. Calc. for $C_{20}H_{32}F_6N_4CrP$ (525.47 g/mol): C, 45.72; H, 6.14; N, 10.66. Found: C, 45.68; H, 6.08; N, 10.64%. EPR-data see text.

### 3.4. {[1,4-(Me₂N)₂-η⁶-C₆H₄]₂Cr}I (5⁺·I⁻)

To a solution of **5** (200 mg, 0.57 mmol) in 30 ml of Et$_2$O were added dropwise 5 ml of a 0.25 M solution of methyl iodide in Et$_2$O. A red precipitate formed, which was collected and washed with Et$_2$O. The product was dissolved in MeCN. Upon gradually reducing the volume in the cold, carmine red crystals of $5^{+\cdot}$I$^-$ are obtained, which are suitable for X-ray diffraction. They are highly air sensitive, forming a blue surface layer immediately on contact with air.

Anal. Calc. for $C_{20}H_{32}CrN_4I$ (507.40 g mol$^{-1}$): C, 47.34; H, 6.36; N, 11.04. Found: C, 47.54; H, 6.19; N, 11.21%.

## 4. Crystallography

Single crystals of **4** and $5^{+\cdot}$I$^-$ were mounted on a glass fiber in a drop of inert oil and frozen in the cold nitrogen stream of the cooling device. The diffraction experiments were carried out at 213 K on a Siemens P4 four circle diffractometer using graphite-monochromated Mo–K$_\alpha$-radiation. Cell parameters and orientation matrix for both complexes were obtained from least squares refinement of 30 accurately centered high angle reflections. No crystal decay was observed during the data collection. The structures were solved by direct methods (**4**) and Patterson methods ($5^{+\cdot}$I$^-$) respectively [24]. Structure refinements were made on $F^2$ values by the full-matrix least-squares technique [25]. All non-hydrogen atoms were refined with anisotropic displacement parameters. A refinement of **4** in the controsymmetric space group $C2/c$ was not successful Other experimental details and the crystal data are summarized in Table 4.

## 5. Supplementary material

Crystallographic data for the structural analysis have been deposited with the Cambridge Crystallographic

Table 4
Summary of crystal structure data for **4** and **5$^+$I$^-$**

|  | **4** | **5$^+$I$^-$** |
|---|---|---|
| Empirical formula | $C_{24}H_{48}CrN_4Si_4$ | $C_{20}H_{32}CrIN_4$ |
| Formula weight | 557.02 | 507.40 |
| Temperature (K) | 213(2) | 213(2) |
| Wavelength (Å) | 0.71073 | 0.71073 |
| Crystal system | Monoclinic | Orthorhombic |
| Space group | $Cc$ | $Pbca$ |
| $a$ (Å) | 26.929(4) | 14.644(2) |
| $b$ (Å) | 6.2900(10) | 15.079(2) |
| $c$ (Å) | 19.509(2) | 19.228(4) |
| $\beta$ (°) | 103.820(10) | |
| $Z$ | 4 | 8 |
| $V$ (Å$^3$) | 3208.8(8) | 4245.9(12) |
| $D_{calc}$ (Mg m$^{-3}$) | 1.153 | 1.588 |
| $\mu$ (mm$^{-1}$) | 0.524 | 2.004 |
| $F(000)$ | 1200 | 2056 |
| Crystal size (mm) | $0.3 \times 0.3 \times 0.1$ | $0.25 \times 0.21 \times 0.18$ |
| $\theta$ range (°) | 2.15–23.01 | 2.12–20.00 |
| Index ranges | $-1 \leq h \leq 28$, $-1 \leq k \leq 6$, $-21 \leq l \leq 20$ | $0 \leq h \leq 14$, $0 \leq k \leq 14$, $0 \leq l \leq 18$ |
| Reflections collected | 2493 | 3286 |
| Independent reflections | 2286 [$R_{int} = 0.0289$] | 1983 [$R_{int} = 0.0773$] |
| Observed reflections | 2008 [$I > 2\sigma(I)$] | 1175 [$I > \sigma(I)$] |
| Reflections used for refinement | 2286 | 1983 |
| Treatment of hydrogen atoms | Located, isotropic refinement | Geometrically, riding model |
| Flack parameter | $-0.02(5)$ | |
| Largest difference peak and hole (e Å$^{-3}$) | 0.586 and $-0.219$ | 0.781 and $-1.112$ |
| Data/restraints/parameters | 2286/2/312 | 1983/0/243 |
| Goodness-of-fit on $F^2$ | 0.996 | 0.835 |
| $wR_2$ (all data) | 0.0943 | 0.1178 |
| $R_1$ (observed data) | 0.0367 | 0.0493 |

Data Centre, CCDC nos. 206443 and 206442 for compounds **4** and **5$^+$·I$^-$**. Copies of this information may be obtained free of charge from The Director, CCDC, 12 Union Road, Cambridge CB2 1EZ, UK (Fax: +44-1223-336033, or e-mail: deposit@ccdc.cam.ac.uk or www: http://www.code.cam.ac.uk).

## References

[1] J. Organomet. Chem. 641 (2002) 208.

[2] U. Nickel, Chem. Zeit 12 (1978) 89.

[3] (a) J.R. Bolton, A. Carrington, J. Dos Santos-Veiga, Mol. Phys. 5 (1962) 615;
(b) D.D. Thomas, H. Keller, H.M. McConnell, J. Chem. Phys. 39 (1963) 2321.

[4] (a) M.R. Bryce, Chem. Soc. Rev. 20 (1991) 355;
(b) J.B. Torrance, Acc. Chem. Res. 12 (1979) 79;
(c) J.L. Segura, N. Martin, Angew. Chem. Int. Ed. 40 (2001) 1372;
(d) K. Pigon, K. Lorenz, Roczniki Chem. 40 (1966) 699, 703;
(e) H. Kusakawa, N. Nishizaki, Bull. Chem. Soc. Jpn. 38 (1965) 2201.

[5] (a) G.T. Pott, J. Kommandeur, J. Chem. Phys. 47 (1967) 395;
(b) Y. Sato, Bull. Chem. Soc. Jpn. 43 (1979) 2370;
(c) J.S. Miller, A.J. Epstein, Angew. Chem. Int. Ed. 33 (1994) 385.

[6] (a) J.W. Eastman, G. Engelsma, M. Calvin, J. Am. Chem. Soc. 84 (1962) 1339;
(b) I. Isenberg, S.L. Baird, J. Am. Chem. Soc. 84 (1962) 3803;
(c) P.H. Emslie, T.J. Thomson, Rec. Trav. Chim. 83 (1964) 1311;
(d) N.H. Kolodny, K.W. Bowers, J. Am. Chem. Soc. 94 (1972) 1113.

[7] (a) G.R. Knox, Proc. Chem. Soc. London (1959) 56;
(b) G.R. Knox, P.L. Pauson, J. Chem. Soc. (1961) 4615.

[8] M. Herberhold, M. Ellinger, W. Kremnitz, J. Organomet. Chem. 241 (1983) 227.

[9] A. Shafir, M.P. Power, G.D. Whitener, J. Arnold, Organometallics 19 (2000) 3978.

[10] (a) H. Plenio, D. Burth, Angew. Chem. Int. Ed. Engl. 34 (1995) 800;
(b) H. Plenio, D. Burth, Organometallics 15 (1996) 4054 (and references cited therein).

[11] C. Elschenbroich, S. Hoppe, B. Metz, Chem. Ber. 126 (1993) 399.

[12] V. Graves, J.J. Lagowski, Inorg. Chem. 15 (1976) 577.

[13] H. Brunner, H. Koch, Chem. Ber. 115 (1982) 65.

[14] A. Shafir, M.P. Power, G.D. Whitener, J. Arnold, Organometallics 20 (2001) 1365.

[15] A.D. Hunter, L. Shilliday, W.S. Furey, M.J. Zaworotko, Organometallics 11 (1992) 1550.

[16] (a) J.L. de Boer, A. Vos, Acta Crystallogr. Ser. B 28 (1972) 835;
(b) J.L. de Boer, A. Vos, Acta Crystallogr. Ser. B 28 (1972) 839;
(c) I. Ikemoto, G. Katagiri, S. Nishimura, K. Yakushi, H. Kuroda, Acta Crystallogr. Ser. B 35 (1979) 2264.

[17] Ch. Elschenbroich, E. Bilger, B. Metz, Organometallics 10 (1991) 2823.

[18] R.G. Compton, R. Barghout, J.C. Eklund, A.C. Fisher, S.G. Davies, M.R. Metzler, J. Chem. Soc. Perkin Trans. 2 (1993) 39.

[19] R.J. Markle, J.J. Lagowski, Organometallics 5 (1986) 595.

[20] Ch. Elschenbroich, E. Bilger, J. Heck, F. Stohler, J. Heinzer, Chem. Ber. 117 (1984) 23.

[21] Ch. Elschenbroich, S. Voss, O. Schiemann, A. Lippek, K. Harms, Organometallics 17 (1998) 4417.

[22] W. Hatke, H.W. Schmidt, W. Heitz, J. Polym. Sci. Part A; Polym. Chem. 29 (1991) 1387.

[23] S. Hünig, H. Quast, W. Brenninger, E. Frankenfeld, Org. Synth. Coll. 5 (1973) 1018.

[24] G.M. Sheldrick, SHELXS-97, Program for the Solution of Crystal Structures, University of Göttingen, Göttingen, Germany, 1997.

[25] G.M. Sheldrick, SHELXL-97, Program for the Refinement of Crystal Structures, University of Göttingen, Göttingen, Germany, 1997.